Stratigraphy, petrology, and structure of Precambrian metavolcanic rocks in the Iris district, Gunnison and Saguache counties, Colorado

Abdulkader M. Afifi

1981, pp. 287-292. https://doi.org/10.56577/FFC-32.287

in:

Western Slope (Western Colorado), Epis, R. C.; Callender, J. F.; [eds.], New Mexico Geological Society 32 nd Annual Fall Field Conference Guidebook, 337 p. https://doi.org/10.56577/FFC-32

This page is intentionally left blank to maintain order of facing pages.

STRATIGRAPHY, PETROLOGY, AND STRUCTURE OF PRECAMBRIAN METAVOLCANIC ROCKS IN THE IRIS DISTRICT, GUNNISON AND SAGUACHE COUNTIES, COLORADO

ABDULKADER M. AFIFI*
Department of Geology
Colorado School of Mines
Golden, Colorado 80401

INTRODUCTION

The Iris district occurs within the Iris and Iris NW 7.5 minute quadrangles, 8-16 km southeast of Gunnison, Colorado. The area is underlain by a mass of Proterozoic (^-1700 m.y.) metavolcanic rocks shown as Dubois Greenstone by Hedlund and Olson (this guidebook). A discussion of the regional geology of Proterozoic rocks exposed along the eastern part of the Gunnison Uplift is presented by Hedlund and Olson. Previous mapping in the Iris district was undertaken by Hedlund and Olson (1974) and Olson (1976). The geology and geochemistry of mineralized areas in the Gunnison gold belt are discussed by Drobeck (1980), and Sheridan and others (this guidebook). The aim of this report is to discuss some aspects of the geology of the small area where detailed mapping was undertaken (Afifi, 1981). Despite two generations of foliation development and metamorphism to the epidote amphibolite facies, relict fabrics and lithologies are locally identified with confidence. For this reason, the prefix "meta" often will be dropped from the following descriptions.

Figure 1 is a simplified geologic map of the Iris district. The stratified rocks are informally divided into three formations: lower metasediments, Iris formation, and upper metasediments. The Iris formation consists of pyroclastic and hyaloclastic rocks and is divided into five mappable members. In chronologic order, these are (1) dacitic member, (2) andesite lapilli tuff member, (3) rhyolitic member, (4) Dirigo Gulch (basaltic) member, and (5) alkali feldspar rhyolite member. Figure 2 is a generalized stratigraphic column for the Iris district showing the proposed stratigraphic nomenclature. The layered rocks are intruded by sheets of metagabbro which are probable subvolcanic equivalents to basaltic rocks of the Dirigo Gulch member. The layered rocks and metagabbro sheets are folded into a tight, steeply plunging fold which is called the Iris syncline. Consequently, all bedding and foliation attitudes are steeply dipping.

STRATIGRAPHY

The stratigraphy of the Iris district represents an interplay between episodes of volcanic eruptions and intervals of epiclastic sedimentation, largely by submarine reworking of personal nonindurated volcanic debris. Intervals of quiescence are marked by deposition of ferruginous chert. In the following treatment, the stratified rocks are described based on their principal mode of fragmentation.

Epiclastic Rocks

Epiclastic rocks include the lower metasediments, the upper metasediments, and numerous lenses of wacke and siltstone interbedded with volcanic rocks of the Iris formation. All epiclastic rocks are metamorphosed to a weakly to strongly schistose assemblage of quartz, feldspar, biotite, muscovite, epidote, and magnetite. The content of microcrystalline biotite and muscovite, derived from a pelitic component, is a reflection of original sorting. Based on sedimentary structures, two facies associations are recognized:

(1) Plane and ripple laminated siltstone, mudstone, and fine grained sandstone. These are interpreted as CE turbidites.

(2) Thinly- to thickly-bedded arkosic wacke and pebbly wacke, which commonly display broad basal scours and grading, followed by parallel stratification. These are interpreted as AA or AB turbidites.

Both associations are laterally and vertically mutually gradational. Other primary structures are slump-folded bedding, load structures, and syndepositional listric normal faults. The association of sedimentary structures indicates a submarine fan environment of deposition, with sandstone occupying submarine channels, and siltstone-mudstone forming overbank (channel margin) deposits.

The composition of most sandstones is arkosic wacke. Quartz is subordinate to feldspar in wackes, and both are probably reworked phenocryst fragments. Pebbles are of local rip-up origin. The microcrystalline matrix composed of quartz, feldspar, biotite, muscovite, and epidote represents metamorphic recrystallization of transported vitric ash.

Pyroclastic Rocks

Pyroclastic rocks include the dacitic, rhyolitic, and alkali feldspar rhyolite members of the Iris formation, in addition to minor dacitic pyroclastic rocks interbedded with the lower metasediments. The rocks consist of metamorphosed tuff, lapilli tuff, and tuff-breccia having various proportions of lithic, crystal, and matrix components. In weakly foliated rocks, the matrix component is observed to consist of silicified and recrystallized vitric ash composed of bubble wall shards (fig. 3). The assemblage of phenocryst fragments allows the distinction of three members. The dacitic member has phenocrysts of plagioclase, orthoclase, and magnetite. The rhyolitic member has phenocrysts of plagioclase, orthoclase, quartz, and magnetite. The alkali feldspar rhyolite member has phenocrysts of alkali feldspar (perthitic intergrowth of orthoclase and albite derived from sanidine), quartz, and magnetite. Chemical data indicates that all three members constitute a calc-alkalic dacite-rhyodacite-rhyolite sequence which becomes increasingly felsic with time.

Most lithic fragments in the pyroclastic rocks are rip-up fragments of tuff, chert, or epiclastic rocks which were incorporated during mass transport. Essential fragments consist of aphyric or vitrophyric felsite (fig. 3), and fragments of long-tube pumice (figs. 3, 4).

*Present address: U.S. Geological Survey, P.O. Box 1488, Jeddah, Saudi Arabia.

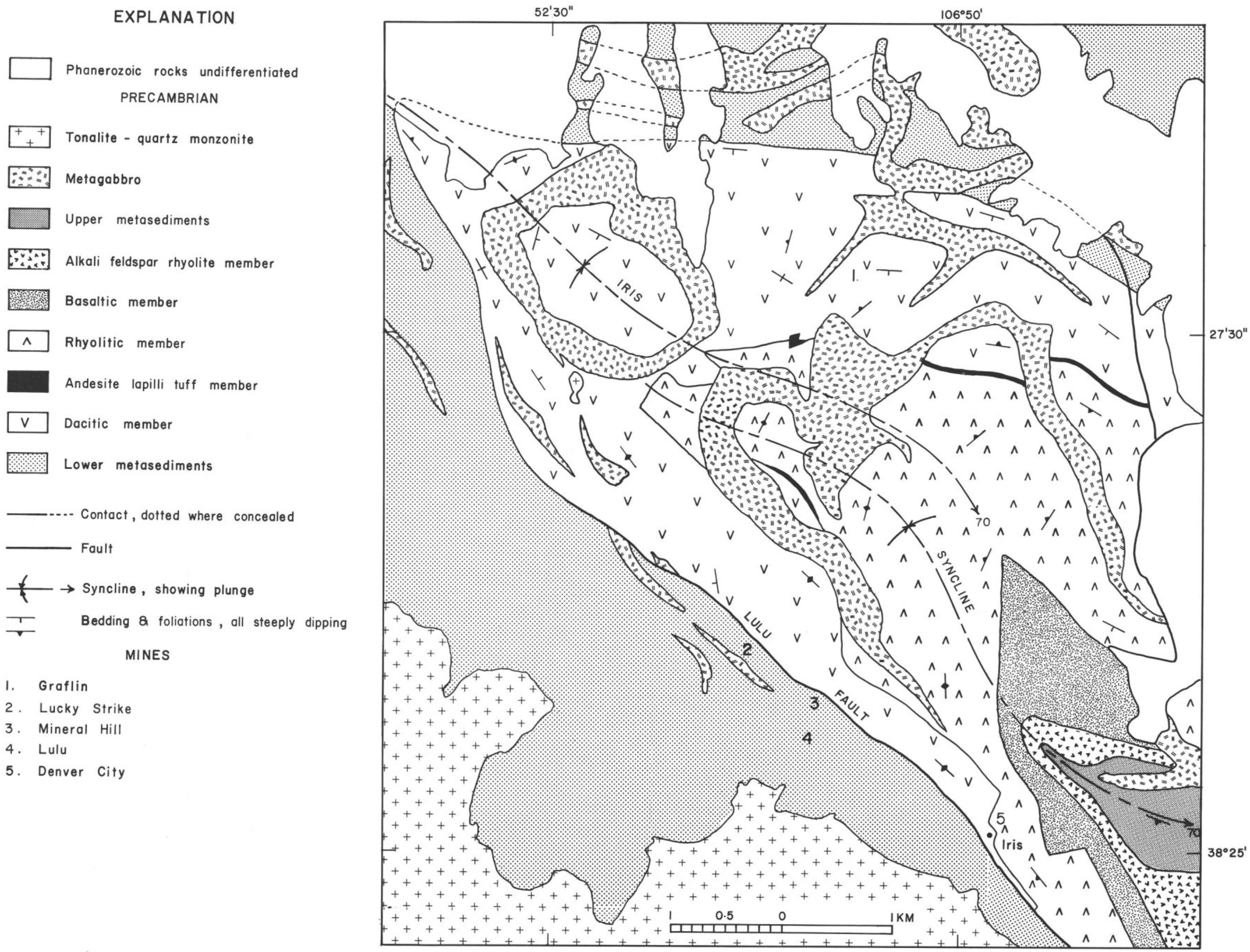

Figure 1. Generalized geologic map of the Iris district, Gunnison and Saguache Counties, Colorado.

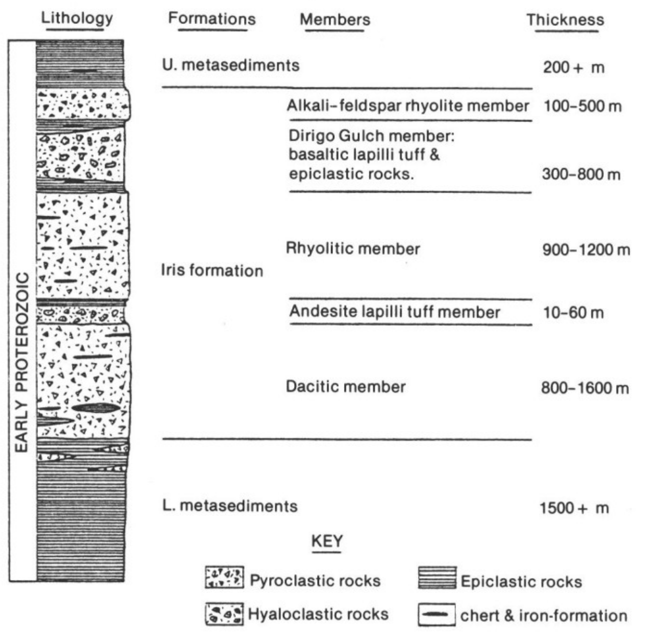

Figure 2. Generalized stratigraphic column for the Iris district. Stratigraphic nomenclature is informal.

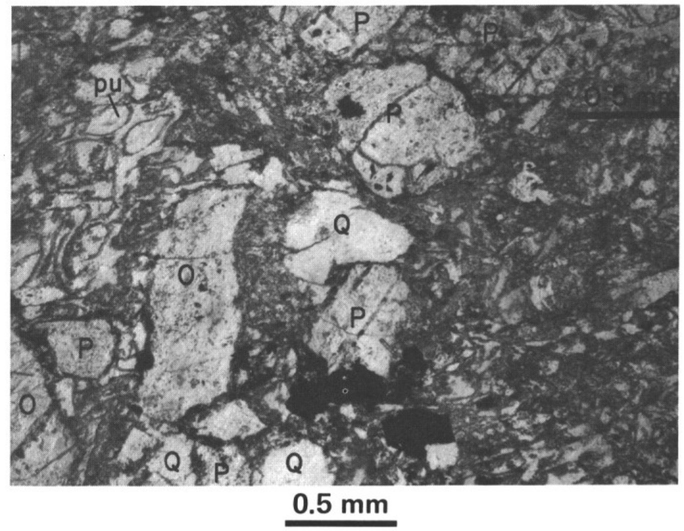

Figure 4. Photomicrograph of nonfoliated quartz latitic lapilli tuff from the rhyolitic member. Fragment to upper left is a cross-sectional view of long-tube pumice (pu). Phenocryst fragments are plagioclase (P), orthoclase (O), quartz (Q), and magnetite (opaque). The matrix consists of bubble wall shards. Shards and pumice are replaced by quartz, and are enveloped by microcrystalline biotite, muscovite, and epidote.

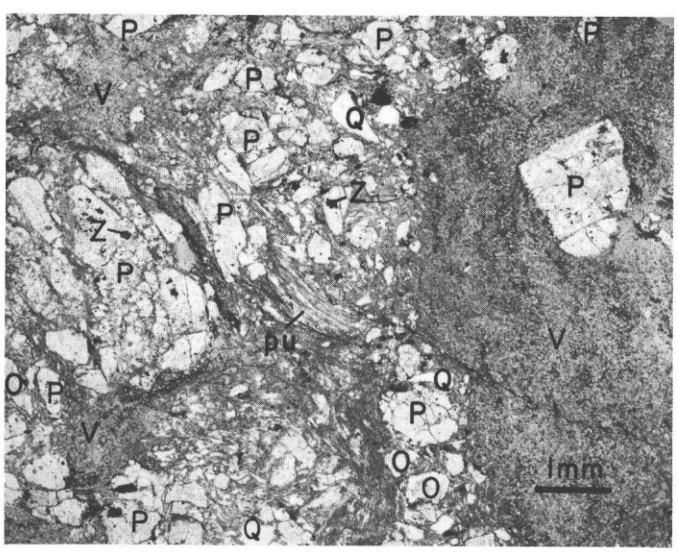

Figure 3. Photomicrograph of nonfoliated quartz latitic lapilli tuff from the rhyolitic member. Uncrossed nicols. Dense fragments are flow banded vitrophyre (V). Phenocrysts and phenocryst fragments are plagioclase (P), orthoclase (O), quartz (Q), magnetite (opaque), and zircon (Z). Matrix consists of long-tube pumice (pu), and shards, both replaced by quartz. The vitric component is metamorphosed into microcrystalline quartz, feldspar, biotite, muscovite, epidote, and magnetite.

Although the pyroclastic rocks rarely display stratification in out crop, detailed study of their primary structures indicates subaque ous deposition by mass-flow mechanisms as described by Middle ton and Hampton (1973). The pyroclastic flows of the Iris distric arrived by a combination of turbulent flow, debris flow, and fluid ized flow mechanisms. Individual pyroclastic flows have scourer bases and locally abundant rip-up fragments of underlying de posits. The typical vertical sequence of primary structures is (1) thin basal zone of reverse grading, (2) a middle massive zone, an((3) an upper zone of normal grading. The upper zone sometime! grades into parallel stratified tuff. Thickness of individual unit: varies from 0.5 to 60 m. The extremely thick units are actually fining-upward sequence of pyroclastic flows which arrived in rapic succession, each carrying successively finer material. Such unit: probably correspond to single eruptions. The vertical sequence o primary structures in pyroclastic flow deposits of the Iris area arE similar to subaqueous mass-flow deposits, including the turbiditE facies association (Walker and Mutti, 1973) and subaqueous pyro clastic flow deposits (Fiske, 1963; Fiske and Matsuda, 1964; TassE and others, 1978).

In thick pyroclastic flows, accidental rip-up fragments of wackE and siltstone underwent soft sediment compaction and are flat tened parallel to bedding (fig. 5), and their undersides are indenter by essential vitrophyre or pumice fragments. This compactiona fabric locally resembles the eutaxitic fabric in moderately welder subaerial pyroclastic flow deposits. However, no effects of plastic deformation or welding of shards or pumice were observed in the Iris district.

Hyaloclastic Rocks

Hyaloclastic rocks include the andesite lapilli tuff member, anc basaltic lapilli tuff and tuff-breccia of the Dirigo Gulch member. Ir both members, the metamorphic assemblage is hornblende, albitE or oligoclase, epidote, biotite, magnetite, quartz, and sphene. ThE rocks consist of self-supported fragments of angular, sparsel vesiculated vitrophyric andesite or basalt, and medium- to coarse.

Figure 5. Massive tuff-breccia zone in a pyroclastic flow deposit from the alkali feldspar rhyolite member. Stratigraphic top is to the left. Effects of soft sediment compaction on rip-up clasts of arkosic wacke are: 1) flattening parallel to bedding (S_o), 2) sigmoidal rotation of bedding planes in some clasts, and 3) indentation of the undersides of soft sediment clasts by rigid equant rhyolite fragments (arrows). Phenocryst fragments consist of alkali feldspar and quartz, and are supported by a microcrystalline matrix derived from vitric ash.

Figure 6. Photomicrograph of meta-andesitic lapilli tuff, uncrossed nicols. Fragment to left consists of microcrystalline devitrification products of andesitic vitrophyre, chiefly hornblende, biotite, and iron oxides. This fragment contains flow-aligned plagioclase microlites, and former vesicles (V). Euhedral pyroxene fragment (Px) is recrystallized into blue-green hornblende, and has a thin skin of recrystallized former andesitic glass. Plagioclase fragment (P) is replaced by albite, epidote, hornblende, biotite, and tourmaline (T). The matrix consists of microcrystalline hornblende, biotite, albite, epidote, quartz, and magnetite. From outcrops 650 m west of Mick Homestead.

grained phenocryst fragments (fig. 6). Although all mafic phenocrysts have recrystallized into hornblende, the euhedral outline of whole phenocryst fragments has enabled distinction of the primary phenocryst assemblages. The andesite had abundant plagioclase, with subordinate pyroxene and amphibole phenocrysts. The basalt had abundant coarse-grained pyroxene, with subordinate plagioclase and olivine. Glassy fragments have recrystallized into microcrystalline aggregates of hornblende and iron-oxides. Chemical analysis indicates that the andesite has a calc-alkalic composition while the basalt of Dirigo Gulch is a Mg-rich tholeiite. Both members are underlain by, overlain by, and laterally gradational into epiclastic rocks. Both display abrupt thickness variation which is partly due to localized deposition in small graben bounded by syndepositional normal faults. Locally, large accidental blocks of wacke are incorporated in basaltic tuff-breccia. Since essential fragments are sparsely vesiculated and glassy, fragmentation was probably due to phreatomagmatic explosions and quenching of subaqueously erupted lava. The lack of sorting, abrupt thickness variation, local incorporation of rip-up clasts, and association with turbidites suggest that deposition was by subaqueous mass flow.

Chert Beds

Interbedded with all stratified rocks are lenticular beds of magnetite quartzite metamorphosed from ferruginous chert and cherry iron formation. The unusual amount of grain growth from chert to quartzite is due to bimineralic composition of the rock. Similar grain growth has occurred in itabirite (banded magnetite quartzite) derived from iron formation (Beukes, 1973).

Chert beds range up to 5 m in thickness and 300 m in strike length. The lenticular nature of these beds is due to localized sedimentation in submarine depressions, and, to a lesser extent, subsequent submarine erosion, since rip-up clasts of chert are commonly incorporated in pyroclastic flow deposits.

INTRUSIVE ROCKS

Metagabbro

Amphibolites derived from gabbroic sills and dikes occur throughout the layered sequence. The larger sills range up to 500 m in thickness. An intrusive origin is indicated by cross-cutting relationships, chilled borders, and relict textures. The outcrop pattern of the larger sills (fig. 1) indicates that they are folded along with the layered sequence. Metagabbros are metamorphosed into blue-green hornblende, albite or oligoclase, epidote, biotite, magnetite, muscovite, and sphene. Where relict textures are preserved, three varieties are recognized: equigranular gabbro, plagioclase-phyric diabase, and pyroxene-phyric basalt. The porphyritic varieties are observed at chilled margins or in dikes. Pyroxene-phyric metabasalt dikes contain hornblende pseudormorphs of coarse-grained euhedral pyroxene phenocrysts which strongly resemble phenocryst fragments in basaltic hyaloclastites of the Dirigo Gulch member. The two rocks are identical in chemistry and are probably co-magmatic.

Large gabbro sills have differentiated in place resulting in metamorphosed differentiates which show a wide range of color index (40-90). Differentiated metadiorites have increasing amounts of plagioclase and biotite at the expense of hornblende. The final differentiates are pods of granophyric albite granite consisting of albite laths and granophyre, with minor magnetite and biotite. This differentiated sequence is similar to that of known layered tholeiitic intrusions. Chemically, equigranular metagabbros are Mg-rich tholeiites. Metadiorites have a higher total FeO/MgO than the metagabbros. The albite granites are chemically similar to keratophyres and plagiogranites.

Granitic Rocks

No subvolcanic granitic rocks are present in the Iris district, but pre-tectonic granitic plutons occur elsewhere in the Gunnison mineral belt (Hedlund and Olson, this guidebook). Post-folding Precambrian intrusions include a stock and cupolas which range in composition from tonalite to quartz monzonite.

STRUCTURAL GEOLOGY

Detailed mapping of stratigraphic units and fabric elements has revealed the existence of the Iris syncline: a major, upright, steeply plunging, tight, disharmonic fold. Due to the local development of several hinges, two synclinal surfaces are located on Figure 1 and are separated by a tight anticlinal flexure. Geometrical analysis of bedding attitudes indicates a plunge of 70° to 85° on an approximate bearing of S40 °E. A consequence of steep plunge is that the geological map (fig. 1) is an approximate tectonic profile of the fold. The Iris syncline displays considerable departure from ideal cylindrical folding because of the large initial variation in the thickness and ductility of stratigraphic units.

Folding of the Iris syncline was accompanied by variable strain which resulted in ductile flattening of lithic fragments into oblate ellipsoids (fig. 7). The earliest foliation (S_1) is defined by the X-Y planes of ellipsoidal fragments, where X, Y, and Z are the maximum, intermediate, and minimum axes of those fragments. The X-axes define the orientation of the L_1 (extension) lineations. Both S_1 and L_1 define the trajectories of strain developed during folding. Figure 8 shows a diagrammatic illustration of S_1 attitudes with respect to the Iris syncline. The S_1 foliation is subparallel to bedding on the limbs, and either subparallel or perpendicular to bedding in the hinge zone. Principal elongation (L_1) is generally perpendicular to the fold axis on the limbs, and subparallel to the fold axis in the hinge zone. The Iris syncline apparently formed by a combination of tangential longitudinal strain and flexural flow mechanisms of buckling.

The lower metasediments on the southwest limb of the Iris syncline have responded to stress by tight isoclinal folding on the mesoscopic scale, resulting in the transposition of bedding. Transposition axes are steeply, but variably plunging due to common overturning of isoclinal folds.

Figure 7. Highly foliated rhyolitic lapilli tuff. Flattened and elongated tuff fragments define the S_1 foliation and the L_1 extension lineation. Later fracture cleavage (S_2) is related to second-generation folding.

The Lulu fault (fig. 1) has a subvertical attitude and cuts upsection through the south limb, bringing successively younger units of the Iris formation in contact with transposed lower metasediments. The Lulu fault is younger than the Iris syncline but older than Precambrian rhyolite dikes which intrude it.

Both the Iris syncline and the Lulu fault have been refolded by an open, steeply plunging, second generation Precambrian fold (fig. 8). The existence of this fold is revealed by the mapping of Olson (1976), but the axial surface occurs largely beneath Tertiary volcanic rocks separating the Iris district from Cochetopa Creek Canyon, 5 km east of the Iris district.

ECONOMIC GEOLOGY

The Iris district contains five abandoned gold mines which were active during the last decade of the nineteenth century (fig. 1). The Denver City Mine, the Graflin Mine, and the Shaunee #33 prospect (500 m east-northeast of the Lulu Mine) are classified as pre-metamorphic deposits based on criteria such as geometry, foliation development, alteration, and metamorphic mineral assemblages. The Denver City Mine is described by Drobeck (this guidebook) and is interpreted as syngenetic in origin. Mineralization at the Graflin Mine consists of foliated veinlets of biotite-pyrite-chalcopyrite and is due to pre-metamorphic fracture filling. The Shaunee #33 prospect is identified as a distal syngenetic massive sulfide occurrence. It consists of a 15-60 cm-thick, stratiform massive sulfide oxidized to hematite-limonite gossan, and has a strike length of 30 m. This deposit occurs conformably within a lens of laminated epiclastic rocks in the dacitic member.

The Mineral Hill Mine, the Lulu Mine, the Lucky Strike Mine, and numerous small occurrences are classified as post-metamorphic epigenetic deposits. Veins consist of quartz-pyrite ± biotite ±

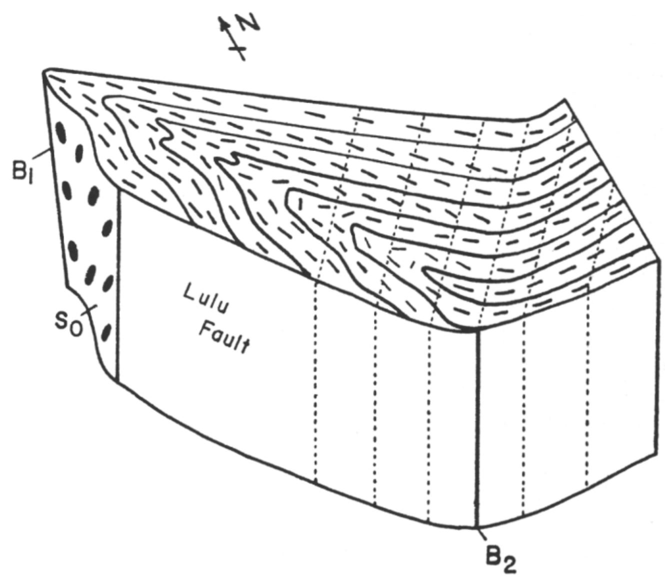

Figure 8. Schematic block diagram showing some principal structural features in the Iris area. The foreground is the surface of the Lulu fault. The Iris syncline (B_1) plunges steeply southeast within the Iris area. Second generation folding has resulted in open refolding of the Iris syncline and the Lulu fault about a steeply plunging axis (B_2). Solid lines represent bedding (S_o), dashed lines represent S_1, and the dotted lines represent fracture cleavage (S_2). The L_1 lineation is defined by elongated ellipsoidal fragments, the traces of which are shown on the S_o surface.

sericite ± tourmaline ± carbonate ± fluorite. These deposits are spatially, and probably genetically, related to a Precambrian post-tectonic tonalite to quartz monzonite stock which occurs in the southern part of the district (fig. 1).

CONCLUSIONS

The available data from detailed studies in the Iris district allow reconstruction of the following sequence of events:

1. Deposition of turbidites, which became increasingly volcanic in composition with time, signaling the onset of calc-alkaline pyroclastic eruptions.
2. Eruptions of voluminous dacitic to rhyodacitic pyroclastic debris and deposition of subaqueous pyroclastic flow deposits.
3. Phreatomagmatic eruption of andesitic hyaloclastite, coinciding with the appearance of quartz phenocrysts in the calc-alkaline magma chamber.
4. Eruptions of voluminous quartz latitic to rhyolitic pyroclastic debris and deposition as subaqueous pyroclastic flow deposits.
5. Intrusion of large tholeiitic gabbro sills and differentiation in place to produce mafic cumulates and felsic liquids.
6. Phreatomagmatic eruption of tholeiitic basaltic hyaloclastite.
7. Pyroclastic eruptions of alkali feldspar rhyolites, which represent the final differentiates of the calc-alkaline magma, and deposition by subaqueous pyroclastic flow mechanisms.
8. Cessation of volcanism and resumption of epiclastic sedimentation.

The entire sequence was deposited largely by mass flow on a submarine slope. Eruptions were subaerial or under shallow water, and deposition was probably at shallow depth. Epiclastic rocks were deposited between eruptions largely by reworking of unconsolidated tuffs. Short quiet intervals are marked by chemical deposition of exhalites, consisting of oxide facies cherry iron formation, or syngenetic massive sulfides.

The predominance of volcanic detritus indicates deposition in an environment of oceanic volcanism, comparable to primitive Phanerozoic island arcs.

Volcanism and sedimentation occurred prior to the Boulder Creek orogeny, c.a. 1700 m.y. ago (Hansen and Peterman, 1968). Two episodes of folding are recognized, and both are correlated with the Boulder Creek orogeny, c.a. 1700 m.y. ago. The earlier generation was one of tight folding around a steeply plunging axis, and resulted in considerable horizontal shortening by internal ductile strain. This episode roughly coincided with prograde metamorphism to the epidote amphibolite facies. The Lulu fault formed after the first folding episode. The second folding episode resulted in open, regional refolding of previous structures.

Post-folding intrusions are calc-alkalic stocks of tonalite to quartz monzonite, with associated rhyolite dikes. These were probably emplaced during the Siller Plume event, c.a. 1400 m.y. ago (Hansen and Peterman, 1968).

The rocks of the Iris area are considered representative of all rock types in the Gunnison Precambrian terrain, excluding pre-folding calc-alkalic intrusions. Such intrusions occur elsewhere in the Gunnison Precambrian terrain and consist of foliated stocks of equigranular to porphyritic grandiorite to leucogranite. Some of these rocks are probable subvolvanic equivalents to pyroclastic rocks in the Iris area. It is indeed impossible to have volcanic rocks without their subvolcanic feeders, and the large volume of pyroclastic rocks in the Iris area suggest derivation from large, shallow, subvolcanic intrusions.

The recognition that the metavolcanic "pile" in the Iris area is a major syncline has led to reinterpretation of the regional structure. The outcrop pattern in the Gunnison Precambrian terrain is an interference pattern due to complex polyphase deformation. The felsic metavolcanic mass in the Iris NW quadrangle, 8 km southwest of the Iris area, is now recognized as a steeply plunging refolded major isoclinal fold.

The stratigraphic relationships established for the Iris area may apply to more deformed rocks in the Gunnison Precambrian terrain. The intermediate to felsic metavolcanic rocks are considered favorable hosts for Zn-Cu volcanogenic massive sulfide deposits.

On a more regional scale, rocks of the Iris area are very similar to Precambrian rocks of the Salida area, 70 km to the east, which have been described by Boardman (1976, 1980a, 1980b). Such similarity provides some insight on the nature of the Precambrian basement of Colorado.

ACKNOWLEDGMENTS

I wish to thank R. C. Epis, G. S. Holden, L. G. Closs, and J. C. Olson for their guidance and assistance. This study benefitted from discussions with P. A. Drobeck and W. D. Reismeyer.

REFERENCES

Afifi, A. M., 1981, Precambrian geology of the Iris area, Gunnison and Saguache Counties, Colorado (M.S. thesis): Golden, Colorado School of Mines, 197 p.

Beukes, N. J., 1973, Iron-formations of southern Africa: Economic Geology, v. 68, p. 960-1004.

Boardman, S. J., 1976, Geology of the Precambrian metamorphic rocks of the Salida area, Chaffee County, Colorado: Mountain Geologist, v. 13, p. 89-100.

, 1980a, Evidence for two stages of Precambrian metamorphism in the Salida area, central Colorado (abs.): Geological Society of America, Abstracts with Programs, v. 12, p. 267.

, 1980b, Geochemistry and origin of Proterozoic amphibolites from Salida, Colorado (abs): Geological Society of America, Abstracts with Pro-, grams, v. 12, p. 268.

Drobeck, P. A., 1980, Geology and trace element geochemistry of a part of the Gunnison Gold Belt, Colorado (M.S. thesis): Golden, Colorado School of Mines, 180 p.

, 1981, Proterozoic syngenetic massive sulfide deposits in the Gunnison gold belt, Colorado: New Mexico Geological Society Guidebook 32, this volume.

Fiske, R. S., 1963, Subaqueous pyroclastic flows in the Ohanapecosh Formation, Washington: Geological Society of America Bulletin, v. 74, p. 391-406.

Fiske, R. S. and Matsuda, T., 1964, Submarine equivalents of ash flows in the Tokiwa Formation, Japan: American Journal of Science, v. 262, p. 76-106.

Hansen, W. R. and Peterman, Z. E., 1968, Basement rock geochronology of the Black Canyon of the Gunnison, Colorado: U.S. Geological Survey Professional Paper 600-C, p. 80-90.

Hedlund, D. C. and Olson, J. C., 1974, Geologic map of the Iris NW Quadrangle, Gunnison and Saguache Counties, Colorado: U.S. Geological Survey Map GQ-1134, 1:24,000.

, 1981, Precambrian geology along parts of the Gunnison uplift of southwestern Colorado: New Mexico Geological Society Guidebook 32, this volume.

Middleton, G. V. and Hampton, M. A., 1973, Sediment gravity flows: mechanics of flow and deposition, *in* Turbidites and deep water sedimentation: SEPM Pacific section short course, p 1-38.

Olson, J. C., 1976, Geologic map of the Iris Quadrangle, Gunnison and Saguache Counties, Colorado: U.S. Geological Survey Map GQ-286, scale 1:24,000.

Tasse, N., Lajoie, J., and Dimroth, E., 1978, The anatomy and interpretation of an Archean volcaniclastic sequence, Quebec: Canadian Journal of the Earth Sciences, v. 15, p. 874-888.

Walker, R. G. and Mutti, E., 1973, Turbidite facies and facies associations, *in* Turbidites and deep water sedimentation: SEPM Pacific Section short course, p. 119-185.